Testing exotic electron-electron interactions with the helium ionization-energy anomaly

Lei Cong,[1,2,3] Filip Ficek,[4,5,*] Rinat Abdullin, Mikhail G. Kozlov,[†] and Dmitry Budker[1,2,3,6]

[1]*Helmholtz Institute Mainz, 55099 Mainz, Germany*
[2]*GSI Helmholtzzentrum für Schwerionenforschung GmbH, 64291 Darmstadt, Germany*
[3]*Johannes Gutenberg University, Mainz 55128, Germany*
[4]*Faculty of Mathematics, University of Vienna, Oskar-Morgenstern-Platz 1, 1090 Vienna, Austria*
[5]*Gravitational Physics Group, University of Vienna, Währinger Straße 17, 1090 Vienna, Austria*
[6]*Department of Physics, University of California at Berkeley, Berkeley, California 94720-7300, USA*

(Received 19 February 2026; revised 28 April 2026; accepted 7 October 2026; published 5 November 2026)

Precision atomic spectroscopy provides a sensitive probe of physics beyond the Standard Model. A recently reported 9σ theory-experiment discrepancy in the ionization energy of metastable helium has motivated the hypothesis of a new boson mediating exotic electron-electron interactions. Using a general sign-consistency analysis of the induced energy shifts, we show that the sign requirement alone excludes vector-vector and pseudoscalar-pseudoscalar interactions as possible explanations of the anomaly. Incorporating existing constraints together with independent limits obtained in this work further excludes axial-vector scenarios. Within the single-boson framework considered in this work, only a narrowly constrained scalar-mediated interaction remains viable. The remaining parameter space could be probed in several different ways—for example, by modest improvements in the determination of the electron gyromagnetic ratio.

DOI: 10.1103/djwc-193y

I. INTRODUCTION

The pursuit of physics beyond the Standard Model (BSM) is motivated by several well-established open questions in fundamental physics, including the origin of the matter-antimatter asymmetry, the nature of dark matter and dark energy, and the hierarchy problem [1–4]. Among the various experimental approaches proposed to probe BSM physics [5–7], precision atomic spectroscopy has emerged as a powerful low-energy probe, complementary to high-energy collider searches, linking high-accuracy measurements to possible new interactions beyond the SM. In particular, simple few-body atomic systems such as hydrogen [8], positronium [9], and helium [10,11] provide exceptionally clean testbeds. As experimental and theoretical uncertainties continue to shrink, these systems are becoming increasingly capable of revealing statistically significant discrepancies that may point either to unknown SM effects or to new physics beyond it.

In this context, helium now stands out as a particularly compelling case. Its spectroscopy has long served as a cornerstone of experimental [12–15] and theoretical [16–21] quantum physics, enabling stringent tests of quantum electrodynamics [22] and the determination of fundamental constants [13]. A long-standing agreement between theory and experiment has recently been challenged by the report of a 9σ discrepancy in the ionization energy of the metastable 2^3S_1 state of ^{4}He [14,19,23,24], which has now also been observed in ^{3}He [15,23]. The persistence of the anomaly across the two isotopes has therefore been discussed as a possible indication of new physics [25].

Building on this observation, we note that the comparable magnitude of the discrepancies in ^{4}He and ^{3}He strongly disfavors explanations rooted in nuclear structure, since the helion and the alpha particle differ substantially in their composition and spin. In particular, finite-size nuclear effects have been excluded as the origin of the anomaly in Ref. [26]. The absence of a large isotope-dependent variation therefore disfavors generic electron-nucleon explanations, unless the proton and neutron couplings are strongly different, and motivates us to search for exotic electron-electron interactions in helium (see Fig. 1).

From the perspective of new-boson searches, the emergence of a discrepancy at the 9σ level marks a qualitative turning point. The anomaly is now sufficiently large that the sign of any proposed new-physics contribution (see more in

*Contact author: filip.ficek@univie.ac.at
†Contact author: mihailgkozlov@gmail.com

Published by the American Physical Society under the terms of the Creative Commons Attribution 4.0 International license. Further distribution of this work must maintain attribution to the author(s) and the published article's title, journal citation, and DOI.

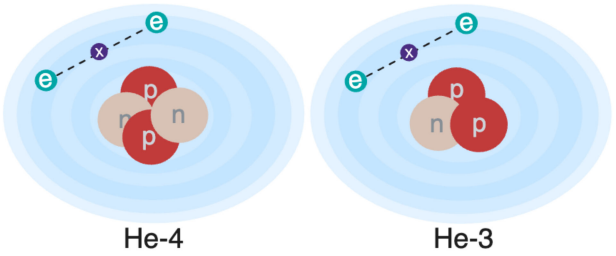


FIG. 1. Schematic illustration of the assumed exotic interaction, mediated by a new boson (X), between electrons within ^{4}He and ^{3}He. Only electron-electron exotic interactions are considered, as they are expected to generate nearly isotope-independent leading-order energy shifts. The shaded regions indicate schematic electron probability distributions.

the Method and Result sections) becomes a decisive consistency criterion, rather than a subleading detail. This opens a fundamentally different strategy to testing exotic interactions, going beyond the incremental tightening of existing bounds [6].

In this work, we take the reported helium discrepancy at face value and perform a stringent test of the single-boson hypothesis. We establish a sign-consistency criterion that becomes decisive at the 9σ level. We compute the exotic-interaction-induced corrections to helium ionization energy for four generic coupling structures—$g_A g_A$, $g_s g_s$, $g_V g_V$, and $g_p g_p$ (where the superscripts indicate axial-vector, scalar, vector, and pseudoscalar couplings). These couplings arise from the exchange of exotic spin-0 and spin-1 bosons, such as axion-like particles and Z' bosons [5,6], between two electrons. We examine whether the *signs* and magnitudes of the couplings can consistently account for the observed deviation. We find that pseudoscalar and vector interactions are immediately excluded by sign inconsistency. A consistent reinterpretation of existing constraints, together with the improved limits obtained in this work, then rules out axial-vector scenarios, leaving a scalar coupling as the only partially viable possibility.

II. THEORY

In this section, we summarize the explicit forms of the exotic electron-electron potentials used in the analysis. We restrict our attention to two classes of bosons considered in this work: a massive spin-1 boson Z' and a spin-0 boson ϕ (e.g., an axion). The analysis is carried out in a general effective-field-theory framework. The corresponding local Lorentz-invariant interactions with a Standard-Model fermion field ψ are given by [6,27–29]

$$\mathcal{L}_{Z'} = Z'_\mu \sum_\psi \bar{\psi}\gamma^\mu (g_V^\psi + \gamma_5 g_A^\psi)\psi, \tag{1}$$

$$\mathcal{L}_\phi = \phi \sum_\psi \bar{\psi}\,(g_s^\psi + i\gamma_5 g_p^\psi)\psi. \tag{2}$$

Here ψ denotes the fermion field ($\psi = e$ for an electron). The dimensionless interaction constants g_s^ψ, g_p^ψ, g_V^ψ, g_A^ψ, parametrize the scalar, pseudoscalar, vector, and axial-vector interaction strengths, respectively.

We group interactions with similar features and identify the dominant terms. In this work we consider four classes: pseudoscalar-pseudoscalar (pp), vector-vector (VV), axial-vector–axial-vector (AA), and scalar-scalar (ss). The relevant exotic potentials are spin-dependent V_{AA}, V_{pp}, and V_{VV}:

$$V_{pp} = \underbrace{-g_p^e g_p^e \frac{\hbar^3}{16\pi c m_e^2}\left[\boldsymbol{\sigma}_e\cdot\boldsymbol{\sigma}'_e\left(\frac{1}{r^3}+\frac{1}{\lambda r^2}+\frac{4\pi}{3}\delta(\boldsymbol{r})\right)-(\boldsymbol{\sigma}_e\cdot\hat{\boldsymbol{r}})(\boldsymbol{\sigma}'_e\cdot\hat{\boldsymbol{r}})\left(\frac{3}{r^3}+\frac{3}{\lambda r^2}+\frac{1}{\lambda^2 r}\right)\right]e^{-r/\lambda}}_{V_3|_{pp}}, \tag{3}$$

$$V_{VV} = \underbrace{g_V^e g_V^e \frac{\hbar c}{4\pi}\frac{e^{-r/\lambda}}{r}}_{V_1|_{VV}} + \underbrace{g_V^e g_V^e \frac{\hbar^3}{16\pi c m_e^2}\left[\boldsymbol{\sigma}_e\cdot\boldsymbol{\sigma}'_e\left[\frac{1}{r^3}+\frac{1}{\lambda r^2}+\frac{1}{\lambda^2 r}-\frac{8\pi}{3}\delta(\boldsymbol{r})\right]-(\boldsymbol{\sigma}_e\cdot\hat{\boldsymbol{r}})(\boldsymbol{\sigma}'_e\cdot\hat{\boldsymbol{r}})\left(\frac{3}{r^3}+\frac{3}{\lambda r^2}+\frac{1}{\lambda^2 r}\right)\right]e^{-r/\lambda}}_{V_2+V_3|_{VV}}, \tag{4}$$

$$V_{AA} = \underbrace{-g_A^e g_A^e \frac{\hbar c}{4\pi}\boldsymbol{\sigma}_e\cdot\boldsymbol{\sigma}'_e\frac{1}{r}e^{-r/\lambda}}_{V_2|_{AA}} \underbrace{-g_A^e g_A^e \frac{\hbar c}{4\pi}\lambda^2\left[\boldsymbol{\sigma}_e\cdot\boldsymbol{\sigma}'_e\left[\frac{1}{r^3}+\frac{1}{\lambda r^2}+\frac{4\pi}{3}\delta(\boldsymbol{r})\right]-(\boldsymbol{\sigma}_e\cdot\hat{\boldsymbol{r}})(\boldsymbol{\sigma}'_e\cdot\hat{\boldsymbol{r}})\left(\frac{3}{r^3}+\frac{3}{\lambda r^2}+\frac{1}{\lambda^2 r}\right)\right]e^{-r/\lambda}}_{V_3|_{AA}}, \tag{5}$$

and spin-independent V_{ss}:

$$V_{ss} = \underbrace{-g_s^e g_s^e \frac{\hbar c}{4\pi}\frac{e^{-r/\lambda}}{r}}_{V_1|_{ss}}, \tag{6}$$

where $\hbar$ is the reduced Planck constant; c is the speed of light in vacuum; $\boldsymbol{\sigma}_e$ and $\boldsymbol{\sigma}'_e$ are vectors of Pauli matrices representing the spins $\boldsymbol{s}_i = \hbar\boldsymbol{\sigma}_i/2$ of the two electrons; m_e is the electron mass; M is the new boson mass, which is inversely proportional to the force range λ, $M = \hbar/(c\lambda)$; and r is the distance between the two electrons.

While we retain the conventional V_i labels [29], it should be emphasized that experimental constraints should, in general, be derived for the underlying boson coupling by considering all potential terms generated by the same interaction simultaneously [6,30]. Treating individual potentials independently is justified only when the different contributions can be experimentally distinguished [31]. An important example is provided by the axial-vector interaction. If one considers $V_2|_{AA}$ alone, the coupling required by the helium anomaly appears viable over a certain range of parameter space. However, when the complete V_{AA} interaction is taken into account, especially the corresponding $V_3|_{AA}$ term, which contains an additional factor of λ^2 [6,27,32–34], this substantially enhances the sensitivity to axial-vector couplings. This distinction plays a key role in the interpretation of the axial-vector scenario considered below. A more detailed discussion can also be found in the Supplemental Material [35].

III. METHOD

To extract the coupling strength of a hypothetical new boson from the theory-experiment discrepancy observed in the ionization energy of the 2^3S_1 state of helium, we interpret the discrepancy as arising entirely from an exotic interaction. The corresponding energy shift is obtained by evaluating the matrix element of the exotic potential using the electronic wave function [11,17,24,36–40] of this state,

$$E^{\text{exotic}} = \langle \Psi_{2^3S_1} | V_i | \Psi_{2^3S_1} \rangle. \tag{7}$$

The adopted wave function

$$\Psi_{2^3S_1,M_J}(\mathbf{r}_1,\mathbf{r}_2) = \psi_S(\mathbf{r}_1,\mathbf{r}_2)\chi_{1,M_J}(1,2) \tag{8}$$

consists of the spatial wave function $\psi_S(\mathbf{r}_1,\mathbf{r}_2)$ and the symmetric triplet spin function $\chi_{1,M_J}(1,2)$ (further details are provided in the Supplemental Material [35]). It has been benchmarked against calculations based on relativistic two-electron wave functions [37,41] and found to provide sufficient accuracy for the present analysis.

The resulting shift can be written in the form $E^{\text{exotic}} = g^e g^e C(\lambda)$, where the overall magnitude is fixed by the difference between the most recent experimental and theoretical determinations,

$$\Delta E = E_{\text{exper}} - E_{\text{theor}} = \mu \pm L, \tag{9}$$

where μ denotes the central value of the discrepancy and L represents the combined experimental and theoretical uncertainty at the 95% confidence level (CL), defined through

$$\int_{-L}^{+L} \frac{1}{\sqrt{2\pi}\sigma} e^{-x^2/(2\sigma^2)} dx = 0.95. \tag{10}$$

Under this interpretation, the corresponding coupling strength is given by $g^e g^e = \Delta E/C(\lambda)$. In the present case, we extract the coupling strength from the upper and lower bounds, $\mu \pm L$ (see Table I), and display it as a band corresponding to this; see Figs. 2 and 3.

On the other hand, recent improvements in measurements of the hyperfine structure of helium [57] and of the fine-structure intervals [54,58] enable a precise determination of the 2^3S_1–2^3P_0 transition (see Table I). In this case, theoretical predictions and experimental results are in excellent agreement, allowing substantially stronger constraints to be set than in earlier studies [11]. See Refs. [11,30,33,59] and the Supplemental Material [35] for details on the derivation of the constraints.

IV. RESULTS

We first show that sign consistency alone already excludes two of the four generic coupling structures, independent of any quantitative constraints. In particular, pseudoscalar- and vector-mediated exotic electron-electron interactions are incompatible with the observed

TABLE I. Theoretical and experimental inputs for calculating ΔE. The relevant ionization energies and transition frequencies are listed; ionization energies are given relative to the ionization threshold, such that bound-state energies are negative. μ = Expt − Theory, $\sigma = \sqrt{\sigma_{\text{th}}^2 + \sigma_{\text{expt}}^2}$. The quantity L is derived from the integral equation; see Eq. (10). For the new-boson case, $\Delta E = \mu \pm L$. For comparison with theory, statistical and systematic uncertainties are combined in quadrature.

Parameter	Theory (kHz)	Exp (kHz)	μ (kHz)	σ (kHz)	ΔE (kHz)
^{4}He 2^3S_1	−1 152 842 742 231(52) [19]	−1 152 842 742 708.2(60) [14]	−477	52	−477 ± 102
^{3}He 2^3S_1	−1 152 788 844 133(52) [18,19,52]	−1 152 788 844 615.4(81) [15]	−482	53	−482 ± 103
2^3S_1-2^3P_0	276 764 094 677(54) [18,19,53][a]	276 764 094 712.45(0.86) [54][b]	35	54	125

[a] See Supplemental Material [35] for the calculation of the theoretical values used.
[b] Earlier experiments [55,56] (not present) yield constraints that are stronger by a factor of 1.2 [55] and weaker by a factor of 1.5 [56], respectively.

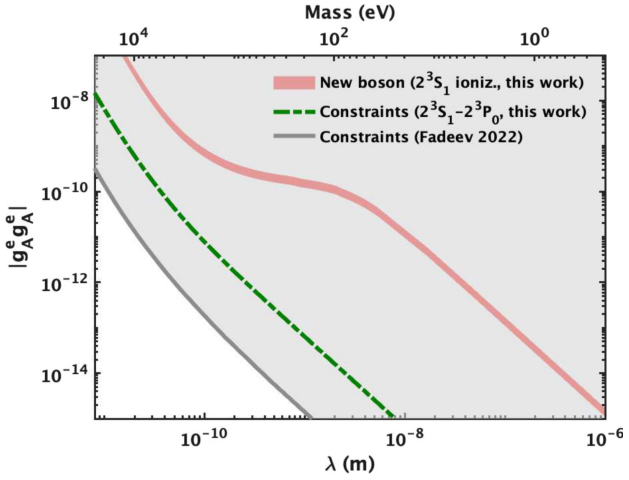


FIG. 2. Axial-vector new-boson coupling product $g_A^e g_A^e$ inferred from the ^{4}He discrepancy (pink band), shown together with existing constraints (gray curves) and the new constraints obtained in this work (green dash-dotted curves) as a function of the interaction range λ (bottom axis). The corresponding boson mass M is shown on the top axis. The corresponding band from ^{3}He is nearly identical and omitted for clarity. For an axial-vector boson, the coupling implied by the helium discrepancy is excluded by constraints obtained in this work, in combination with previous limits from Ref. [33]. Other weaker constraints, such as those from Refs. [42,43], can be found in Refs. [6,44].

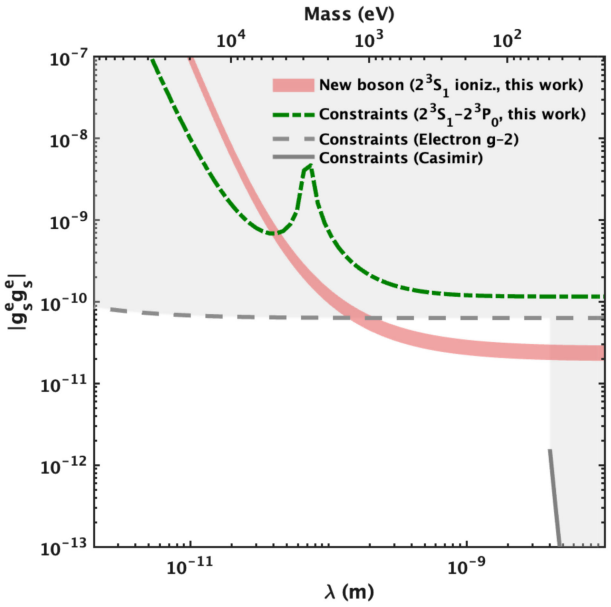


FIG. 3. Scalar new-boson coupling product $g_s g_s$ inferred from the helium discrepancy (pink band), shown together with the constraints obtained in this work (green dash-dotted curve) as a function of the interaction range λ. Gray dashed and solid lines denote the electron $g-2$ [10,45] and Casimir constraints [6,46], respectively. The former is an updated version of the constraint from Refs. [10,45,47], incorporating the latest theoretical [48] and experimental [49] inputs (further details are provided in the Supplemental Material [35]). The corresponding boson mass M is shown on the top axis. In this case, the coupling implied by the helium discrepancy remains possible for $50 < M < 1200$ eV, while the higher-mass range is excluded by existing and new constraints. A cross-check with anomalies in other helium transitions [19,50,51] can be found in the Supplemental Material [35].

helium-ionization-energy discrepancy. This conclusion follows from a simple but decisive observation. For electron-electron exotic interactions, the relevant couplings enter only through their squares, $g_A^{e\,2}$, $g_p^{e\,2}$, g_s^{e2}, and $g_V^{e\,2}$, which are strictly positive. As a result, each exotic potential contributes with a fixed sign that is uniquely determined by its operator structure. Since the measured and theoretical energies satisfy $E^{\text{exper}} = E^{\text{theory}} + E^{\text{exotic}}$, the helium data in Table I require E^{exotic} to be negative. This sign requirement immediately rules out pseudoscalar interactions and vector-type potentials of the $V_1 + V_2 + V_3|_{VV}$ form, whose predicted shifts have the opposite sign.

In earlier analyses of exotic interaction constraints, such as Ref. [11], theory-experiment differences were much smaller and dominated by combined uncertainties spanning both signs, rendering the sign of the exotic contribution effectively irrelevant. Here, by contrast, the much larger 9σ discrepancy elevates sign consistency to a decisive criterion.

Having eliminated pseudoscalar and vector scenarios by sign consistency alone, we next examine whether the remaining axial-vector [6,27,32–34] and scalar interactions [6,28,60–63] are compatible with existing experimental constraints.

These results are summarized in Figs. 2 and 3. In both figures, the pink bands denote the coupling strengths required to account for the helium discrepancy, as extracted from ^{4}He data. The corresponding coupling band inferred from ^{3}He is shifted by approximately 1% relative to the ^{4}He central value, while its width is nearly identical to that of the ^{4}He band, differing below the 10^{-3} level; it lies slightly above the ^{4}He curve and is therefore not shown for clarity. The dash-dotted green curves indicate the new constraints obtained in this work, while the gray curves represent existing direct or indirect bounds.

Figure 2 demonstrates that an axial-vector boson explanation of the helium discrepancy is incompatible with the constraints based on combined exotic potentials. Because a physical axial-vector mediator generically induces all allowed axial-axial interaction terms, the relevant limits must be evaluated for the full combined potential $V_2 + V_3|_{AA}$ [6,30,33,64] rather than for individual contributions (further details are provided in the Supplemental Material [35]). Accordingly, Fig. 2 compares the coupling required to explain the helium discrepancy with constraints derived from the combined $V_2 + V_3|_{AA}$ interaction. The new bounds from the 2^3S_1–2^3P_0 transition (see Table I) obtained in this work and the previously established limits [33] both exclude this scenario entirely.

We now turn to the spin-independent scalar interaction. In this case, the induced energy shift has the same sign as the observed discrepancy and therefore survives the sign-consistency test. Using a wave function for the 2^3S_1 state from Refs. [11,17], we find that, for a scalar mediator with $M < 1200$ eV, the coupling strength required to reproduce the reported discrepancy lies below existing bounds, leaving room for a possible explanation of the discrepancy.

More specifically, Fig. 3 shows that a spin-independent scalar boson is reduced to $M < 5000$ eV by our newly obtained constraints (dash-dotted green line) from the 2^3S_1–2^3P_0 helium transition. Some constraints reported in Ref. [10] were based on older theoretical values and are therefore not shown here, in light of the updated results of Ref. [19]. To further narrow the possible mass window for a new boson, we also show the improved electron $g-2$ constraint [10,48,49] (further details are provided in the Supplemental Material [35]) and Casimir constraints [6,46,65] for scalar bosons in Fig. 3. These bounds further exclude a scalar-boson explanation of the helium discrepancy, leaving it possible only for $50 < M < 1200$ eV. Comparisons with state-of-the-art helium wave-function calculations [41] show that improvements to the electronic wave function lead only to modest changes in the relevant matrix elements (see the Supplemental Material [35]), which is insufficient to qualitatively alter the conclusions presented above.

We note, however, that the electron $g-2$ constrains new physics [66,67] in a conceptually different manner from fifth-force searches. In helium spectroscopy, a new boson is treated as being exchanged between two electrons, giving rise to an effective exotic potential [6], whereas in the $g-2$ measurement it enters through virtual loop corrections to the electron-photon vertex [10,68,69]. As a result, the corresponding $g-2$ bounds are subject to the assumed ultraviolet completion of the interaction and are therefore not directly equivalent to constraints from fifth-force experiments. Nevertheless, improved determinations of the electron gyromagnetic ratio provide a particularly promising test of the remaining scalar parameter space. Astrophysical and cosmological probes [70–73], such as observations of red-giant (RG) and horizontal-branch (HB) stars, constrain the electron-scalar coupling to $g_s^e \sim 10^{-15}$ [6,74], approximately 10 orders of magnitude below the coupling suggested by the helium anomaly. Such constraints can, however, be evaded in extended models; for example, additional interactions can make the effective particle mass increase in dense stellar environments, suppressing its production while leaving its laboratory phenomenology accessible [75,76]. See the Supplemental Material [35] for further discussion. Therefore, further direct constraints on $g_s^e g_s^e$, for example from high-precision measurements of other helium transitions or nano-opto-mechanical sensors [77], remain highly desirable.

V. CONCLUSION AND OUTLOOK

Assuming that the reported 9σ helium ionization-energy discrepancy originates from new physics, we have shown that the sign of the required energy shift provides a decisive criterion for testing candidate exotic electron-electron interactions. This sign-consistency criterion rules out entire classes of single-boson explanations: pseudoscalar-pseudoscalar ($g_p g_p$) and vector-vector ($g_V g_V$) couplings generate shifts of the wrong sign. The axial-vector case ($g_A g_A$) is also excluded when the full $V_2 + V_3|_{AA}$ potential and existing constraints are treated consistently.

A scalar interaction ($g_s g_s$) remains the only partially viable scenario: our new constraints from the 2^3S_1–2^3P_0 helium transition restrict the allowed region to $M < 5000$ eV, while the improved electron $g-2$ limits further restrict it to $M \lesssim 1200$ eV. Overall, the observed discrepancy is strongly disfavored as a signal of a new single boson, except possibly for a light scalar mediator with $50 < M < 1200$ eV within the single-boson, single-coupling framework considered here.

Although our analysis leaves a limited scalar new-boson parameter window open, this interpretation must be carefully distinguished from possible missing higher-order QED contributions. The theoretical ionization energies in Table I include complete QED contributions through order $m\alpha^7$ [19]. The dominant remaining theoretical uncertainty arises from the uncalculated $m\alpha^8$ contribution, which was estimated in Ref. [19] using hydrogenic results for He^+, with a 30% uncertainty assigned to the estimate. This results in an uncertainty of approximately 52 kHz for the theoretical 2^3S_1 ionization energy [24], substantially smaller than the observed ~0.5 MHz discrepancy. Nevertheless, because this uncertainty is based on an estimate rather than a complete two-electron calculation, an explicit calculation of the $m\alpha^8$ contribution in helium would provide an important test of whether the discrepancy can originate from presently uncalculated QED effects.

Looking ahead, a variety of experimental platforms may further test and potentially exclude the remaining scalar new-boson parameter space. Precision positronium spectroscopy, as proposed in Ref. [78], provides a concrete testbed for investigating the helium ionization-energy anomaly. At the same time, high-precision experimental and theoretical studies of the triplet spectrum of Li^+ are under active development and offer another promising avenue [79]. In addition, even modest improvements in the determination of the electron gyromagnetic ratio would provide a powerful test of the remaining scalar-boson parameter space. Beyond the single-boson electron-electron framework considered here, it would also be interesting to investigate whether electron-proton interactions could account for the observed discrepancies, although such scenarios are subject to strong existing constraints [8,80–83]

and would likely require additional model assumptions or finely-tuned cancellations.

More broadly, the present work illustrates a general framework for interpreting statistically significant anomalies in precision measurements by combining independent precision observables into a unified consistency test of new-physics scenarios. Within this framework, once an anomaly reaches sufficient significance, the sign of the required new-physics contribution can provide an additional powerful discriminator among competing explanations. This framework can be extended beyond helium to future anomalies in atomic, molecular, and other precision probes of new physics [5–7,84–87].

ACKNOWLEDGMENTS

The authors acknowledge helpful discussions with Frederick Merkt, Gordon Drake, Yotam Soreq, Yevgeny Stadnik, Vladimir Yerokhin, Gilad Perez, Surjeet Rajendran, Dmitry Glazov, Egor Lazarev, Robert Potvliege, and Shui-Ming Hu. This work has been supported by the Cluster of Excellence "Precision Physics, Fundamental Interactions, and Structure of Matter" (PRISMA++ EXC 2118/2) funded by the German Research Foundation (DFG) within the German Excellence Strategy (Project ID 390831469) and by the COST Action within the project COSMIC WISPers (Grant No. CA21106). L. Cong acknowledges support from the Deutsche Forschungsgemeinschaft (DFG, German Research Foundation) under Project No. 578071833. F. F. acknowledges the support of the Austrian Science Fund (FWF) via Project No. PAT 9429324 (DOI:10.55776/PAT9429324). R. A. and M. K. were supported by the Foundation for the Advancement of Theoretical Physics and Mathematics "BASIS."

DATA AVAILABILITY

The data that support the findings of this article are openly available [44], embargo periods may apply.

[1] M. Dine and A. Kusenko, Rev. Mod. Phys. **76**, 1 (2003).
[2] J. L. Feng, Annu. Rev. Astron. Astrophys. **48**, 495 (2010).
[3] P. W. Graham, D. E. Kaplan, and S. Rajendran, Phys. Rev. Lett. **115**, 221801 (2015).
[4] S. Navas *et al.* (Particle Data Group), Phys. Rev. D **110**, 030001 (2024).
[5] M. S. Safronova, D. Budker, D. DeMille, D. F. J. Kimball, A. Derevianko, and C. W. Clark, Rev. Mod. Phys. **90**, 025008 (2018).
[6] L. Cong, W. Ji, P. Fadeev, F. Ficek, M. Jiang, V. V. Flambaum, H. Guan, D. F. Jackson Kimball, M. G. Kozlov, Y. V. Stadnik, and D. Budker, Rev. Mod. Phys. **97**, 025005 (2025).
[7] A. Arza, D. Aybas, S. Balaji, R. Balkin, K. Bartnick *et al.*, arXiv:2603.03433.
[8] S. G. Karshenboim, Phys. Rev. Lett. **104**, 220406 (2010).
[9] G. Adkins, D. Cassidy, and J. Pérez-Ríos, Phys. Rep. **975**, 1 (2022).
[10] C. Delaunay, C. Frugiuele, E. Fuchs, and Y. Soreq, Phys. Rev. D **96**, 115002 (2017).
[11] F. Ficek, D. F. J. Kimball, M. G. Kozlov, N. Leefer, S. Pustelny, and D. Budker, Phys. Rev. A **95**, 032505 (2017).
[12] H. A. Schuessler, E. N. Fortson, and H. G. Dehmelt, Phys. Rev. **187**, 5 (1969).
[13] Y. R. Sun and S.-M. Hu, Natl. Sci. Rev. **7**, 1818 (2020).
[14] G. Clausen, K. Gamlin, J. A. Agner, H. Schmutz, and F. Merkt, Phys. Rev. A **111**, 012817 (2025).
[15] G. Clausen and F. Merkt, Phys. Rev. Lett. **134**, 223001 (2025).
[16] M. Born, R. J. Blin-Stoyle, and J. M. Radcliffe, *Atomic Physics* (Dover Publications, New York, 1989).
[17] H. A. Bethe and E. E. Salpeter, *Quantum Mechanics of One- and Two-Electron Atoms* (Springer, Berlin, Heidelberg, 2013).
[18] K. Pachucki, V. V. Patkóš, and V. Yerokhin, Phys. Rev. A **95**, 062510 (2017).
[19] V. V. Patkóš, V. A. Yerokhin, and K. Pachucki, Phys. Rev. A **103**, 042809 (2021).
[20] G. W. F. Drake, in *Springer Handbook of Atomic, Molecular, and Optical Physics*, edited by G. W. F. Drake (Springer International Publishing, Cham, 2023), pp. 199–216.
[21] G. Drake, in *Springer Handbook of Atomic, Molecular, and Optical Physics* (Springer, New York, NY, 2006), pp. 199–219.
[22] R. J. Rengelink, Y. van der Werf, R. P. M. J. W. Notermans, R. Jannin, K. S. E. Eikema, M. D. Hoogerland, and W. Vassen, Nat. Phys. **14**, 1132 (2018).
[23] G. B. Clausen, Precision spectroscopy in ^{3}He and ^{4}He: Rydberg states and ionization energies, Ph.D. thesis, ETH Zurich, Zurich, Switzerland, 2025.
[24] G. W. F. Drake, A. T. Bondy, O. P. Hallett, and B. C. Najem, Phys. Rev. A **113**, 012810 (2026).
[25] A. T. Bondy, Physics **18**, 110 (2025).
[26] K. Steinebach, J. C. J. Koelemeij, H. L. Bethlem, and K. S. E. Eikema, Phys. Rev. Lett. **136**, 243001 (2026).
[27] P. Fadeev, Y. V. Stadnik, F. Ficek, M. G. Kozlov, V. V. Flambaum, and D. Budker, Phys. Rev. A **99**, 022113 (2019).
[28] J. E. Moody and F. Wilczek, Phys. Rev. D **30**, 130 (1984).
[29] B. A. Dobrescu and I. Mocioiu, J. High Energy Phys. 11 (2006) 005.
[30] L. Cong, F. Ficek, P. Fadeev, and D. Budker, Phys. Rev. A **112**, 052824 (2025).
[31] D. W. P. Amaral, L. Cong, T. M. Fuchs, H. Ulbricht, and D. Budker, arXiv:2606.30781.
[32] L. Cong, F. Ficek, P. Fadeev, Y. V. Stadnik, and D. Budker, arXiv:2503.07161.

[33] P. Fadeev, F. Ficek, M. G. Kozlov, D. Budker, and V. V. Flambaum, Phys. Rev. A **105**, 022812 (2022).
[34] S. G. Karshenboim, Phys. Rev. A **83**, 062119 (2011).
[35] See Supplemental Material at http://link.aps.org/supplemental/10.1103/djwc-193y for details on the wave functions, exotic-interaction-induced energy shifts, derivation of constraints, complementary analyses of electron $(g-2)$, other helium transitions, and astrophysical bounds.
[36] K. V. Rodriguez, G. Gasaneo, and D. M. Mitnik, J. Phys. B **40**, 3923 (2007).
[37] S. A. Alexander, S. Datta, and R. L. Coldwell, Phys. Rev. A **81**, 032519 (2010).
[38] J. Chi, H. Fang, Y.-H. Zhang, X.-Q. Qi, L.-Y. Tang, and T.-Y. Shi, Atoms **13**, 72 (2025).
[39] D. T. Aznabaev, Phys. Rev. A **98**, 012510 (2018).
[40] G. W. F. Drake and Z.-C. Yan, Phys. Rev. A **46**, 2378 (1992).
[41] R. Abdullin, E. Lazarev, D. A. Glazov, M. G. Kozlov *et al.*, Relativistic and correlation corrections to exotic electron-electron interactions in helium (tentative title) (unpublished).
[42] M. Jiao, X. Rong, H. Liang, Y.-F. Cai, and J. Du, Phys. Rev. D **101**, 115011 (2020).
[43] S. Kotler, R. Ozeri, and D. F. J. Kimball, Phys. Rev. Lett. **115**, 081801 (2015).
[44] L. Cong, W. Ji, and D. Budker, Spin-dependent fifth force dataset, https://lei-cong.github.io/Spin-Dependent-5th-Force-Limits/ (2025).
[45] D. Hanneke, S. Fogwell, and G. Gabrielse, Phys. Rev. Lett. **100**, 120801 (2008).
[46] M. Bordag, U. Mohideen, and V. M. Mostepanenko, Phys. Rep. **353**, 1 (2001).
[47] T. Aoyama, M. Hayakawa, T. Kinoshita, and M. Nio, Phys. Rev. Lett. **109**, 111807 (2012).
[48] S. Volkov, Phys. Rev. D **100**, 096004 (2019).
[49] X. Fan, T. G. Myers, B. A. D. Sukra, and G. Gabrielse, Phys. Rev. Lett. **130**, 071801 (2023).
[50] C. Dorrer, F. Nez, B. de Beauvoir, L. Julien, and F. Biraben, Phys. Rev. Lett. **78**, 3658 (1997).
[51] P.-L. Luo, J.-L. Peng, J. Hu, Y. Feng, L.-B. Wang, and J.-T. Shy, Phys. Rev. A **94**, 062507 (2016).
[52] K. Pachucki and V. A. Yerokhin, J. Phys. Chem. Ref. Data **44**, 031206 (2015).
[53] K. Pachucki and V. A. Yerokhin, Phys. Rev. Lett. **104**, 070403 (2010).
[54] J.-L. Wen, J.-D. Tang, Y.-N. Lv, Y. R. Sun, C.-L. Zou, J.-F. Dong, and S.-M. Hu, Sci. Adv. **11**, eadu9796 (2025).
[55] P. C. Pastor, G. Giusfredi, P. D. Natale, G. Hagel, C. de Mauro, and M. Inguscio, Phys. Rev. Lett. **92**, 023001 (2004).
[56] D. Shiner, R. Dixson, and P. Zhao, Phys. Rev. Lett. **72**, 1802 (1994).
[57] X. Zheng, Y. R. Sun, J.-J. Chen, W. Jiang, K. Pachucki, and S.-M. Hu, Phys. Rev. Lett. **118**, 063001 (2017).
[58] X. Zheng, Y. R. Sun, J.-J. Chen, W. Jiang, K. Pachucki, and S.-M. Hu, Phys. Rev. Lett. **119**, 263002 (2017).
[59] F. Ficek, P. Fadeev, V. V. Flambaum, D. F. Jackson Kimball, M. G. Kozlov, Y. V. Stadnik, and D. Budker, Phys. Rev. Lett. **120**, 183002 (2018).
[60] U. Mohideen and A. Roy, Phys. Rev. Lett. **81**, 4549 (1998).
[61] D. J. Kapner, T. S. Cook, E. G. Adelberger, J. H. Gundlach, B. R. Heckel, C. D. Hoyle, and H. E. Swanson, Phys. Rev. Lett. **98**, 021101 (2007).
[62] J. C. Long, H. W. Chan, A. B. Churnside, E. A. Gulbis, M. C. M. Varney, and J. C. Price, Nature (London) **421**, 922 (2003).
[63] J. Bergé, P. Brax, G. Métris, M. Pernot-Borràs, P. Touboul, and J.-P. Uzan, Phys. Rev. Lett. **120**, 141101 (2018).
[64] R. Kang and X. Rong, Phys. Rev. D **112**, 115026 (2025).
[65] M. Bordag, G. L. Klimchitskaya, U. Mohideen, and V. M. Mostepanenko, *Advances in the Casimir Effect* (Oxford University Press, New York, 2009), Vol. 145.
[66] J. P. Leveille, Nucl. Phys. **B137**, 63 (1978).
[67] M. Lindner, M. Platscher, and F. S. Queiroz, Phys. Rep. **731**, 1 (2018).
[68] Yu. M. Andreev, D. Banerjee, J. Bernhard, V. E. Burtsev, A. G. Chumakov *et al.* (NA64 Collaboration), Phys. Rev. Lett. **126**, 211802 (2021).
[69] C. Frugiuele, J. Pérez-Ríos, and C. Peset, Phys. Rev. D **100**, 015010 (2019).
[70] G. G. Raffelt, Annu. Rev. Nucl. Part. Sci. **49**, 163 (1999).
[71] J. Jaeckel, E. Massó, J. Redondo, A. Ringwald, and F. Takahashi, Phys. Rev. D **75**, 013004 (2007).
[72] P. Brax, C. van de Bruck, and A.-C. Davis, Phys. Rev. Lett. **99**, 121103 (2007).
[73] P. Jain and S. Mandal, Int. J. Mod. Phys. D **15**, 2095 (2006).
[74] S. Knapen, T. Lin, and K. M. Zurek, Phys. Rev. D **96**, 115021 (2017), 1709.07882.
[75] W. DeRocco, P. W. Graham, and S. Rajendran, Phys. Rev. D **102**, 075015 (2020).
[76] R. Budnik, H. Kim, O. Matsedonskyi, G. Perez, and Y. Soreq, Phys. Rev. D **104**, 015012 (2021).
[77] F. Fogliano, B. Besga, A. Reigue, L. Mercier de Lépinay, P. Heringlake, C. Gouriou, E. Eyraud, W. Wernsdorfer, B. Pigeau, and O. Arcizet, Nat. Commun. **12**, 4124 (2021).
[78] J. Pérez-Ríos and D. B. Cassidy, arXiv:2608.12747.
[79] V. A. Yerokhin, V. V. Patkóš, and K. Pachucki, Phys. Rev. A **107**, 012810 (2023).
[80] M. Moretti, C. H. Keitel, and Z. Harman, Phys. Rev. Lett. **136**, 011803 (2026).
[81] R. M. Potvliege, New J. Phys. **27**, 045002 (2025).
[82] R. M. Potvliege, A. Nicolson, M. P. A. Jones, and M. Spannowsky, Phys. Rev. A **108**, 052825 (2023).
[83] V. Debierre, C. H. Keitel, and Z. Harman, Phys. Lett. B **807**, 135527 (2020).
[84] U. D. Jentschura, Phys. Rev. A **101**, 062503 (2020).
[85] N. Leefer, A. Gerhardus, D. Budker, V. V. Flambaum, and Y. V. Stadnik, Phys. Rev. Lett. **117**, 271601 (2016).
[86] K. Gaul, L. Cong, and D. Budker, Phys. Rev. Lett. **136**, 181805 (2026).
[87] C. J. West and B. M. Roberts, arXiv:2608.26532.